

EFFECTS OF LIGHTWEIGHT MULLITE-SILICA RICH GLASS COMPOSITE AGGREGATES ON PROPERTIES OF CASTABLES

YUANYUAN LI, #NAN LI, WEN YAN

*The Key State Laboratory Breeding Base of Refractories and Ceramics,
Wuhan University of Science and Technology, Wuhan 430081, China*

#E-mail: linanref@yahoo.com.cn

Submitted March 17, 2013; accepted September 27, 2013

Keywords: Lightweight castable, Mullite-silica rich glass composite, Chamotte, Properties

Mullite-silica rich glass (MSRG) composite is a material which is more efficient than chamotte for refractory utilization of clay. The effects of lightweight MSRG composite aggregate on the properties of refractory castables were studied by XRD, SEM and EDS, etc. Comparing with a common lightweight chamotte aggregate, it was found that the hot modulus of rupture, refractoriness under load and thermal shock resistance of the castable with lightweight MSRG aggregate were higher than those of the castable with a common lightweight chamotte aggregate because MSRG did not contain silica crystalline phases and contained a liquid phase with very high viscosity at high temperature. The castables with lightweight chamotte aggregate have higher thermal expansion because of existence of cristobalite and quartz, and have lower thermal conductivity because of higher porosity.

INTRODUCTION

Lightweight aggregate concrete (LWAC) has been widely used in construction. A lot of studies of effects of lightweight aggregate (LWA) on the properties of LWAC have been done. The volume fraction and properties of LWA affect the mechanical properties of LWAC, especially the shape index of LWA has a great influence on the mechanical properties of LWAC [1]. The porous surface of LWA improves the interfacial bond between the aggregate and the cement paste to change the strength of LWAC [2]. The hardened self-consolidating concrete (SCC) with LWA in lower unit weight has lower mechanical and physical properties except for thermal properties when compared to the properties of SCC [3]. The density and mix proportion of LWA give influences on the strength of SCC [4]. Besides mentioned above, there are a lot of papers dealing with the effects of lightweight aggregate on properties of LWAC, such as by Lo et al. [5], Kim et al. [6], Ke et al. [7] and Yan et al. [8-10]. With the increasing requirement of environment and climate, it becomes very important to reduce energy consumption and CO₂ emission of industrial furnace. Refractories as the lining materials play an important role on the reduction of energy consumption and CO₂ emission of industrial furnace. Refractory castables have been widely used in industrial furnace. In order to reduce

the thermal conductivity of the castables, the lightweight aggregates are used in castables, for example, it was used as a tundish permanent lining [11]. However, the studies of effects of LWA on the properties of refractory LWAC have been done little. Because refractory castables are used at high temperature, the properties at elevated temperature, such as refractoriness under load, thermal shock resistance, modulus of rupture at high temperature, thermal expansion and thermal conductivity, are very important. Properties of LWA give strong effects on the properties of LWAC. The lightweight chamotte aggregate is based on clay. It consists of mullite, silica polymorphism and glass phase, as well it has lower thermal shock resistance because of the phase transformation of silica polymorphism during heating and cooling. The MSRG composite is a material which is more efficient than chamotte for refractory utilization of clay [12]. This composite consists of mullite and silica-rich glass, but there are no cristobalite and quartz existing. It is reported that hampering the formation of cristobalite can decrease the temperature coefficient of linear expansion of the binding part and increase the heat resistance of chamotte specimens [13]. In a previous paper, we reported the preparing and properties of lightweight MSRG [14]. In this paper, we deal with the effects of lightweight MSRG aggregate on the properties of castable, comparing with a lightweight chamotte aggregate.

EXPERIMENTAL

Properties of lightweight aggregates

Two lightweight MSRAG aggregates were used in this study, comparing with a common lightweight chamotte aggregate. The chemical compositions and the compositions of crystalline and glass phase of the three aggregates marked as E, F and G are listed in Table 1, 2, 3, respectively. The measure methods of content and composition of crystalline and glass are given in our another paper [12]. Aggregate E and F were MSRAG aggregate and fired in a tunnel kiln at 1500°C and 1620°C, respectively, and aggregate G was common chamotte lightweight aggregate and fired at about 1400°C. There are no data of G in Table 2 and Table 3 because silica polymorphism cannot be separated from glass phase by HF acid treatment.

XRD patterns of three aggregates obtained by X-ray diffractometry (XRD; Model Xpert TMP, Philips, Eindhoven, Netherlands) are given in Figure 1. The main crystalline phase of aggregates E and F are mullite, with a few amount of corundum coexisting. While besides mullite and corundum, there exist cristobalite and quartz in aggregate G.

The apparent porosities, pore sizes of the aggregates and viscosity of the silica-rich glass phase of the aggregates at 1600°C are given in Table 4. The measure methods of viscosity are given in our another paper [14]. The strength of the aggregate was evaluated by the numerical tube pressure, also listed in Table 4. The numerical tube pressure was conducted as follows: Pack aggregates with size of 5 - 4 mm in a Ø 50 mm mould to a height of 50 mm, the mass of aggregates is m_0 , and then press it with a pressure of 50 MPa for 10 seconds; then sift the pressed aggregates by a sieve with a pore size of 3×3 mm; eventually, weigh the mass of the aggregates

with a size bigger than 3 mm as m_1 ; consequently the numerical tube pressure was given by $m_1/m_0 \times 100\%$ [15].

The porosity of sample F is smaller than that of E and the pore size of F are bigger than that of E because sample F was sintered at higher temperature. Among the three samples, G has the least bulk density and highest porosity because of the least Al_2O_3 content and the lowest sintering temperature. Aggregate G has the least numerical tube pressure. It means it has the least strength.

Table 4. Properties of aggregates E, F and G.

	E	F	G
Apparent porosity (%)	47.4	39.8	47.7
Bulk density (g/cm^3)	1.47	1.64	1.35
Pore size ($d_{50}, \mu m$)	33.73	95.3	15.42
Numerical tube pressure (%)	40.2	42.1	30.4
Viscosity of liquids (1600°C, Nsm^{-2})	4197.6	4666.6	–

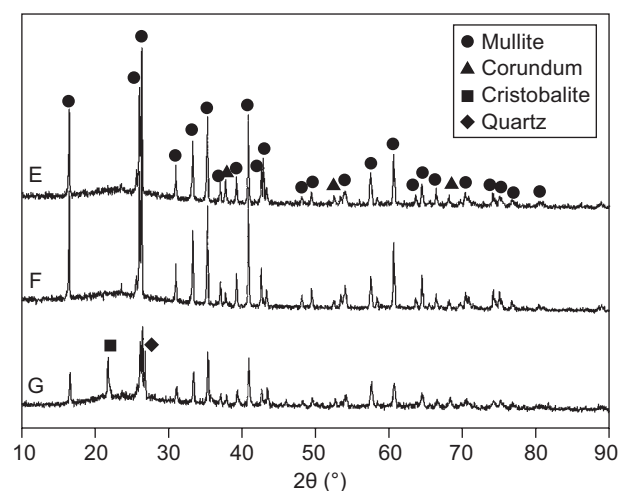


Figure 1. XRD patterns of aggregates.

Table 1. Chemical compositions of lightweight aggregates (wt. %).

	A/S ratio	SiO ₂	Al ₂ O ₃	Fe ₂ O ₃	CaO	MgO	K ₂ O	Na ₂ O	TiO ₂	Glass content
E	1.32	40.02	52.67	1.24	0.77	0.45	1.63	1.41	2.08	34.93
F	1.32	40.10	52.83	1.15	0.72	0.41	1.63	1.06	2.06	35.64
G	1.12	43.25	48.53	3.75	1.22	0.33	0.66	0.10	2.58	–

Table 2. Chemical compositions of the crystalline phases of aggregates (wt. %).

	A/S ratio	SiO ₂	Al ₂ O ₃	Fe ₂ O ₃	CaO	MgO	K ₂ O	Na ₂ O	TiO ₂
E	3.68	20.60	75.82	0.90	0.68	0.29	0.24	0.14	1.30
F	3.36	22.17	74.56	0.63	0.72	0.26	0.29	0.15	1.12

Table 3. Chemical compositions of the glass phases of aggregates (wt. %).

	A/S ratio	SiO ₂	Al ₂ O ₃	Fe ₂ O ₃	CaO	MgO	K ₂ O	Na ₂ O	TiO ₂
E	0.13	75.57	9.47	1.86	0.93	0.74	4.18	3.74	3.50
F	0.19	72.43	13.58	2.09	0.72	0.68	4.05	2.70	3.75

Microstructures of pores of three aggregates were shown in Figure 2. Figure 3 gives the pore size distributions and cumulative distributions of three aggregates obtained by the optical microscope (Axioskop40) and its self-contained image analysis software. Sample G has pores with the least size and uniform distribution.

Microstructures observed by a scanning electron microscope (SEM) (Philips XL30) and energy dispersive X-ray spectroscopy (EDS) analysis processed by EDAX ZAF quantification (standardless) are shown in Figure 4. It is found that the three samples have different mullite crystal size because of different sintering temperature. Sample F has the largest mullite crystal based on the highest sintering temperature and sample G has the least mullite crystal based on the lowest sintering temperature.

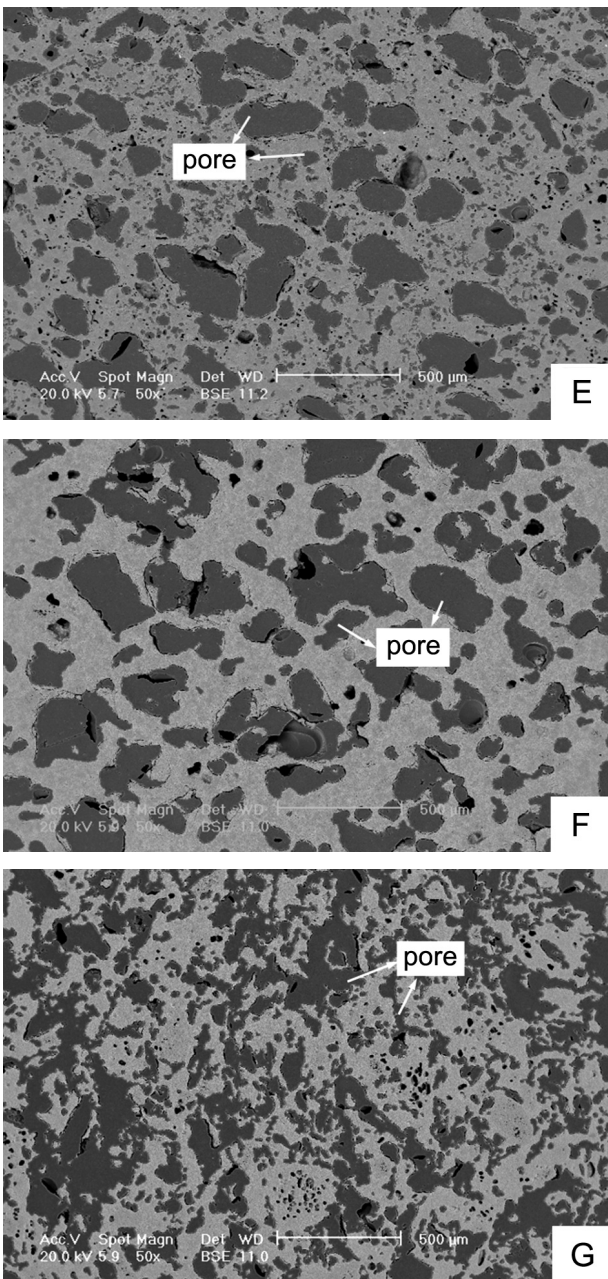


Figure 2. SEM micrographs of aggregates E, F and G.

Comparing with the properties and microstructures of lightweight MSRГ and chamotte aggregates mentioned above, it is found that the differences between these two types of aggregates are not only the phase compositions but also the properties. MSRГ is sintered at higher temperature than chamotte, resulting in the lower porosity, higher strength, larger pore size and larger mullite crystal size, as well as the disappearance of silica polymorphisms. These differences will lead to the differences of the properties of castable with different aggregate.

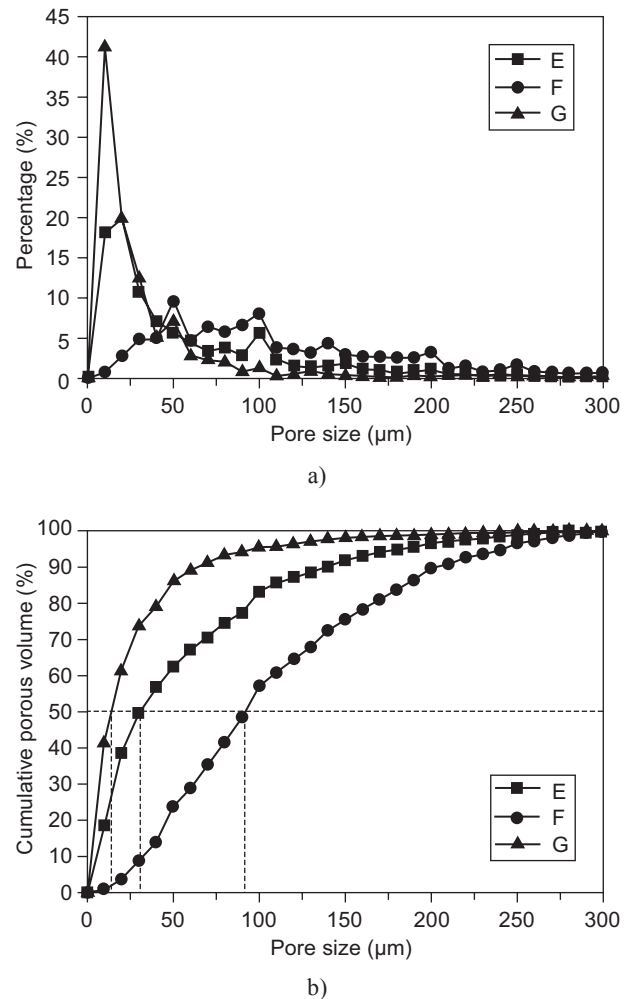


Figure 3. Pore size distributions (a) and cumulative distributions (b) of aggregates E, F and G.

Preparation and properties of castables

The castables were prepared with different lightweight aggregates but the same matrix. Three castables were named as EC, FC and GC according to their corresponding aggregates. The contents of aggregate and powder in the castable mixture were 67 vol. % and 33 vol. %, respectively. 6 % calcium aluminate was used as a binder. The water contents of castables EC, FC and GC were 15 wt. %, 13.1 wt. % and 17.1 wt. %, based on

the different porosity and pore size of different aggregate, respectively. Rectangle parallelepiped specimens of 25×25×140 mm were casted for the porosity, density and strength measurement. The disk specimens with 180 mm diameter and 20 mm thickness were casted for the thermal conductivity test. The rectangle specimens of 40×40×160 mm were casted for thermal expansion tests. A column specimen with Φ50×H50 mm was tested for the refractoriness under load. They were cured 24 h at room temperature and dried at 110°C for 24 h. Specimens were heated at 1200°C for 3 h in an electric chamber furnace and then furnace-cooled to room temperature.

The microstructure of these samples was observed using the SEM. Apparent porosities and bulk densities

of the samples were measured by Archimedes' principle with water as the medium.

For the measurement of the flexural strength after thermal shock, the sintered samples were inserted into a preheated furnace at 950°C for 25 min and then quenched in air. After one thermal shock, the flexural strengths of the quenched samples were measured at room temperature. And the residual flexural strength was given as (flexural strength after thermal shock) ×100 %/ (flexural strength before thermal shock).

The thermal conductivity, hot modulus of rupture at 1250°C, refractoriness under load and thermal expansion of samples refer to Chinese standard YB/T 4130-2005, GB/T 3002-2004, GB/T 5989-2008, and GB/T 7320.1-2000, respectively.

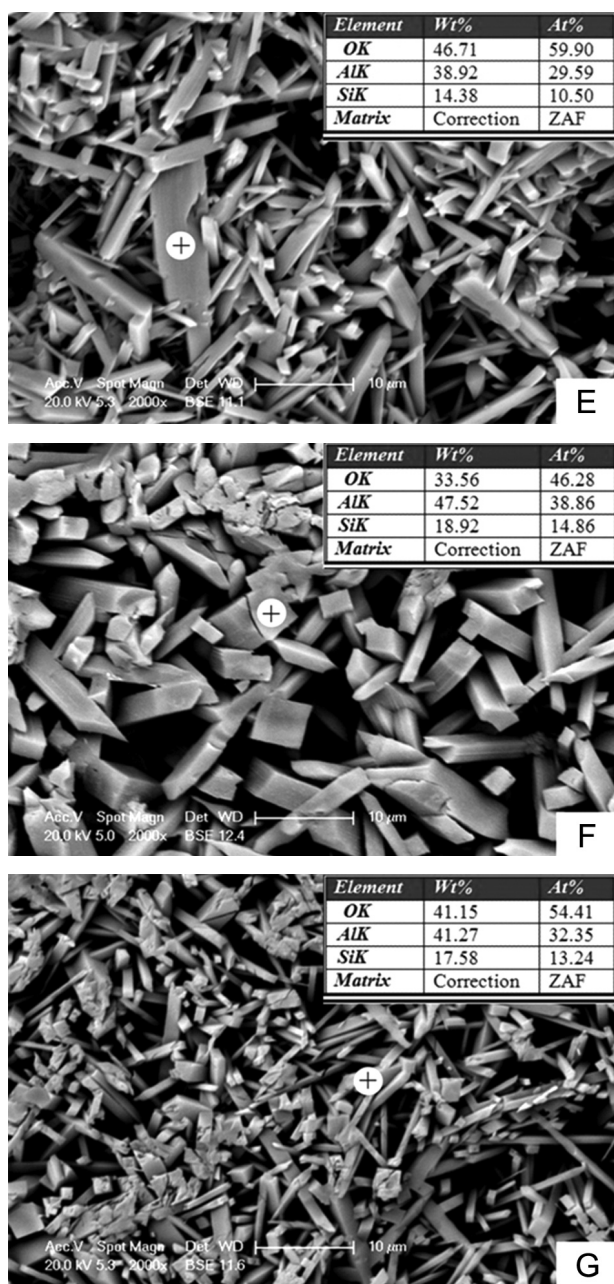


Figure 4. SEM micrographs and EDS analysis of aggregates after HF-etched (+ Mullite).

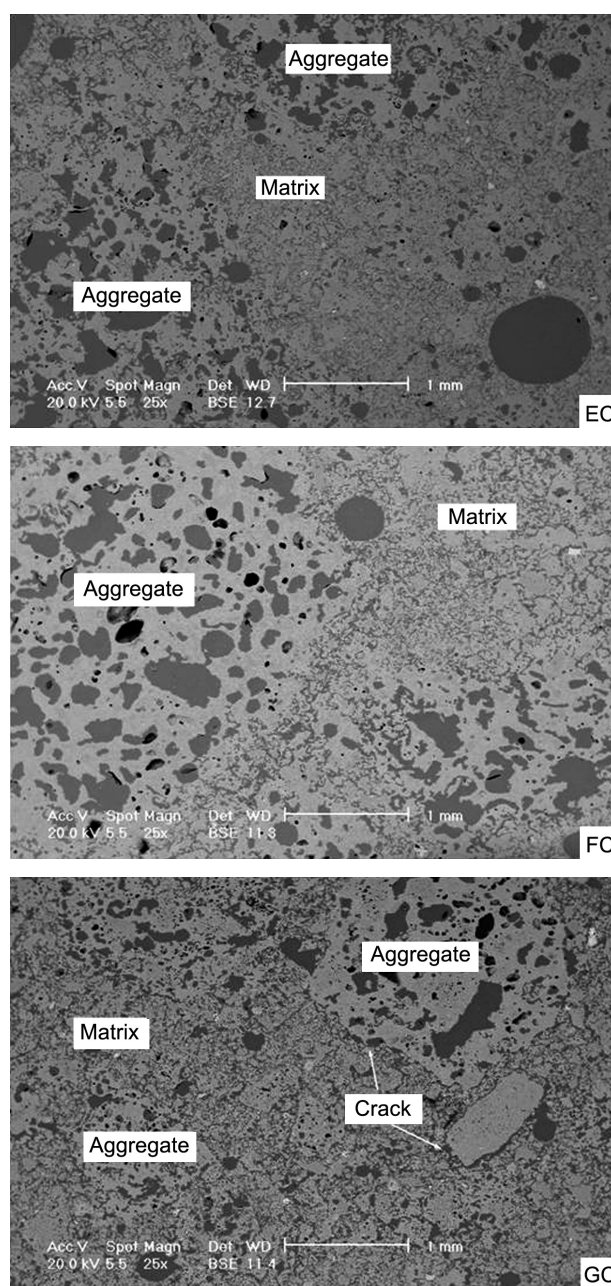


Figure 5. SEM micrographs of castables.

RESULTS AND DISCUSSION

Apparent porosity (AP), bulk density (BD), cold modulus of rupture (CMOR) and cold crushing strength (CCS)

The AP, BD, CMOR and CCS of the three samples are given in Table 5. It is obvious that castable GC has the highest porosity, which results in lower strength. The high porosity of the lightweight chamotte aggregate is a reason of higher porosity of sample GC, another reason may be the formation of cracks resulting from silica polymorphism transformation during cooling. From Figure 5, it is seen that there are cracks between aggregate and matrix in sample GC but in sample EC and FC these cracks are very few.

Table 5. Properties of castables.

		EC	FC	GC
AP (%)	110°C × 24 h	33.2	27.7	34.3
	1200°C × 3 h	34.8	30.0	36.2
BD (g/cm ³)	110°C × 24 h	1.84	1.98	1.76
	1200°C × 3 h	1.83	1.94	1.73
CMOR (MPa)	110°C × 24 h	1.3	1.5	0.8
	1200°C × 3 h	12.0	13.4	9.7
CCS (MPa)	110°C × 24 h	13.5	19.8	10.6
	1200°C × 3 h	63.4	97.2	35.6

Hot modulus of rupture (HMOR), refractoriness under load and thermal shock resistance

Figure 6 and Figure 7 show the hot modulus of rupture and refractoriness under load of the three samples, respectively. Table 6 gives the flexural strength before and after thermal shock and the residual flexural strength of the three samples. It is found that the hot modulus of rupture, refractoriness under load and thermal shock resistance of sample EC and FC which use MSR as aggregates are considerably higher than those of GC which use common lightweight chamotte as aggregate. In the castable mixture, LWA content is of 67 vol. %. LWA aggregates form a framework in the castables and the powder mixture fills in the pores among the aggregates. The phase compositions, microstructures and properties of LWAs give a strong effect on the properties of the castables. The lightweight aggregate E and F consist of mullite and glass rich in silica.

Table 6. Properties of castables before and after thermal shock.

Castables		EC	FC	GC
Flexural strength (MPa)	before thermal shock	18.14	19.07	14.95
	after thermal shock	0.86	1.40	0.67
Residual flexural strength (%)		4.75	7.32	4.51

They are stable at elevated temperature. Contrarily, lightweight aggregate G consists of mullite, glass and silica polymorphism which is not stable at elevated temperature. The transformation of silica polymorphism results in volume change which breaks the structure of aggregates and the framework in the castables, as well as the formation of cracks between aggregate and matrix (Figure 5). On the other hand, the glass of sample E and F have higher SiO₂ content than sample G. At elevated temperature, the viscosity of liquid in sample E and F is higher than that in sample G, and the creep under load of sample E and F should be less than that of sample G. These are the reasons why the hot modulus of rupture, refractoriness under load and thermal shock resistance of sample EC and FC are higher than those of sample GC. Apart from the reasons mentioned above, larger mullite crystal size and lower porosity of lightweight aggregates E and F may be beneficial to improve the properties of castable EC and FC at high temperature.

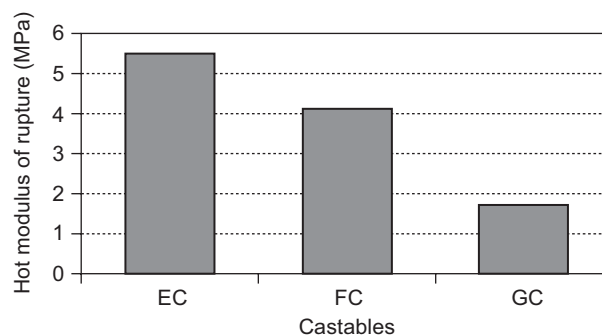


Figure 6. Hot modulus of rupture of castables.

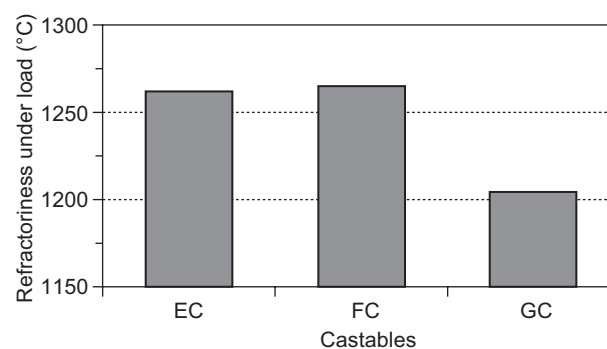


Figure 7. Refractoriness under load of castables.

Thermal conductivity and thermal expansion ($\Delta L/L_0$)

Figure 8 gives the relations between the thermal conductivity of the three castable samples and the temperature. The sample GC has the lower thermal conductivity than the other two samples because GC has higher porosity. Figure 9 gives the relations between the linear expansion ratio $\Delta L/L_0$ and the temperature. The $\Delta L/L_0$ of sample GC is larger than that of sample EC and

FC because cristobalite and quartz exist in aggregate G. The difference among three castables is the aggregates, not the matrix, so the $\Delta L/L_0$ difference of castables mainly comes from the aggregates. For aggregates E and F, they consist of mullite ($5.3 \times 10^{-6}/K$) and silica-rich glass ($0.5 \times 10^{-6}/K$). The two phases both have low coefficient of thermal expansion (CTE), resulting that the aggregates have lower CTE. While for aggregate G, besides mullite and glass phase, it also has cristobalite and quartz ($10 \sim 12 \times 10^{-6}/K$) [16, 17]. On one hand, the higher CTEs of cristobalite and quartz increase the CTE of the sample, on the other hand, the volume expansion from the polymorphism transformation of quartz also increase the CTE of the sample. That is the reason why sample GC has larger thermal expansion than sample EC and FC. When the temperature increases up to $1200^\circ C$, the $\Delta L/L_0$ of sample GC begins to decrease with increase temperature because the formation of liquid improves sintering. However, for sample EC and FC, $\Delta L/L_0$ does not decrease obviously when the temperature increases

up to $1200^\circ C$ because of high viscosity of the liquid in MSRAG aggregates and the sintering is not improved evidently.

CONCLUSION

The MSRAG aggregate gives strong effect on the properties of castables. The hot modulus of rupture, refractoriness under load and thermal shock resistance of castables with lightweight MSRAG aggregates are higher than those of castables with lightweight chamotte aggregate because MSRAG aggregates do not contain cristobalite and quartz but contain a high viscosity liquid at high temperature, and have lower porosity and larger mullite crystal size. The castables with lightweight chamotte aggregate have higher thermal expansion because of existence of cristobalite and quartz, and the castables with lightweight chamotte aggregate have low thermal conductivity because of their higher porosity.

Acknowledgment

The authors would like to thank the 973 Program earlier research project in China (No. 2012CB722702) for financially supporting this work.

REFERENCE

1. Cui H.Z., Lo T.Y., Memon S.A., Xu W.: *Constr. Build. Mater.* 35, 149 (2012).
2. Lo T.Y., Cui H.Z.: *Mater. Lett.* 58, 916 (2004).
3. Topcu I.B., Uygunoglu T.: *Constr. Build. Mater.* 24, 1286 (2010).
4. Kim Y.J., Choi Y.W., Lachemi M.: *Constr. Build. Mater.* 24, 11 (2004).
5. Lo T.Y., Cui H.Z., Tang W.C., Leung W.M.: *Constr. Build. Mater.* 22, 623 (2008).
6. Kim H.K., Jeon J.H., Lee H.K.: *Constr. Build. Mater.* 29, 193 (2012).
7. Ke Y., Beaucour A.L., Ortola S., Dumontet H., Cabrillac R.: *Constr. Build. Mater.* 23, 2821 (2009).
8. Yan W., Li N., Han B.Q.: *Int. J. Appl. Ceram. Tec.* 5, 633 (2008).
9. Yan W., Li N., Han B.Q.: *Sci. Sinter.* 41, 275 (2009).
10. Yan W., Li N., Han B.Q., Fang X.M., Liu G.P.: *Ceram. Silik.* 54, 315 (2010).
11. Luo Z.Y., Liu K.Q., Wang B.J.: *Naihuo Cailiao* 44, 362 (2010).
12. Yan W., Li N., Li Y.Y.: *Appl. Clay Sci.* (In press) (2013).
13. Pilipchatin L.D., Shevtsov R.N., Kozdoba V.I.: *Refract. Ind. Ceram.* 40, 30 (1999).
14. Li Y.Y., Li N., Yan W., Liu G.P.: *Ceram. Silik.* 55, 246 (2011).
15. Yan W., Li N., Miao Z., Liu G.P., Li Y.Y.: *J. Ceram. Process Res.* 13, 278 (2012).
16. Guan Z.D., Zhang Z.T., Jiao J.S.: *Tsinghua University Press* (2004).
17. Li N., Gu H.Z., Zhao H.Z.: *Metallurgical Industry Press* (2010).

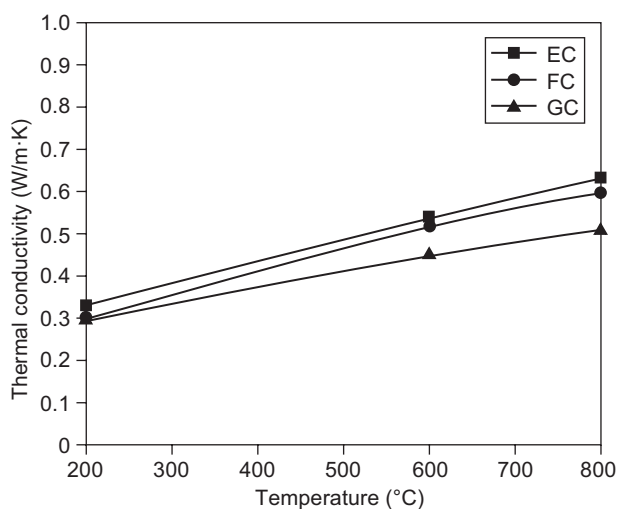


Figure 8. Change of thermal conductivity of castables with heating temperature.

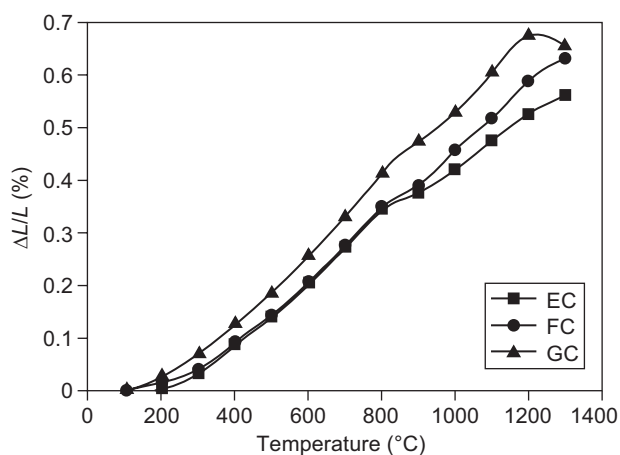


Figure 9. $\Delta L/L_0$ of the castables at different temperature.